COMPUTATIONALLY EFFICIENT EXTRACTION AND INTEGRATION OF MULTI-WAVELET BASED FEATURES FOR SEGMENTATION OF SAR IMAGES

V.V.Chamundeeswari[a,*], D. Singh[a]
[a]Department of Electronics and Computer Engineering, Indian Institute of Technology Roorkee Roorkee- 247 667.
vjcsedec@iitr.ernet.in, dharmfec@iitr.ernet.in

KEYWORDS: M-band wavelet packets, Unsupervised classification, Texture, Intensity feature vectors

ABSTRACT:

Classification of land cover using SAR images is an area of considerable current interest and research. A number of methods have been developed to classify land cover from SAR images and these techniques are often grouped into supervised and unsupervised classification algorithms. Supervised methods have yielded better accuracy but suffer from the need of human interaction to determine the classes. In contrast, unsupervised methods determine classes automatically but limitation with the algorithms developed for this method is that they use multi band or multi polarized data. In this paper, we proposed an algorithm to effectively classify a single band, single polarized image having intensity and texture information only. The proposed algorithm provides the user with the required parameters for direct segmentation process with out any trial and error approach. Classification accuracy for water and urban areas are computed by comparing with LISS image and topographic sheet and quite good agreement is obtained. The algorithm is also evaluated by applying the results to the SAR images obtained at different time instants.

1. INTRODUCTION

The segmentation of different land cover regions is identified as a complex problem. In general, any remotely sensed image may contain water bodies, vegetation, habitation, open spaces etc. but these regions are not very well separated because of low spatial resolution. So, assigning a particular land cover type to every pixel is a genuine problem of remotely sensed images. The active Synthetic Aperture Radar (SAR) enables high-resolution imaging (25m spatial resolution) of the geographic region of interest independent of daylight and cloud cover. Satellite carrying this sensor (European Remote Sensing ERS-1/2) has relatively low temporal resolution and this SAR uses only one polarization and one frequency further limiting detection capabilities. A single band single polarized SAR image contains information only in the form of intensity and texture. An efficient segmentation algorithm to classify SAR images in to different land cover will lead to promising utilization of SAR data.

Different methods have been proposed for the analysis of image texture. Popular methods include those based on grey-level co-occurrence matrix (GLCM) (Haralick *et al*., 1979), Markov random fields (MRFs) (Manjunath *et al*., 1991), Gabor wavelets (Jain *et al.,* 1991; Manjunath *et al.,* 1996), tree structured wavelets (Chang *et al*., 1993), wavelet packets (Clausi *et al.,* 1998), sum-difference histograms etc. see (Randen *et al.,* 1999) for comparative performance of general texture analysis schemes. GLCM provided better classification accuracy only for optical images while semivariogram did better on microwave images. Mecocci *et al.,* 1995 presented a wavelet based algorithm combined with a fuzzy c- means classifier. Lindsay *et al*., 1996 used the one dimensional discrete wavelet transform (DWT) based on Deubechies wavelet filter. M. Acharyya segmented the remotely sensed images using multi wavelet based features (Acharyya, M., *et al.,*2000). All these unsupervised techniques used multi-band, multi-polarized images and user defined parameters to achieve optimum classifications, which is the main limitation of this approach.

Therefore, in this paper, an attempt has been made by proposing an adaptive algorithm to minimize these limitations. We present a methodology to the user so that the segmentation process for a single band single polarized SAR image can be applied directly for optimum classification. This method presented is made computationally efficient based on the notion of approximate features selected with the help of neuro fuzzy network.

2. EXPERIMENTAL DATASETS

2.1 Study Area

Solani river catchment around Roorkee town in the state of Uttaranchal, India has been taken as the study area. The area is relatively flat with elevations ranging from 245.5 meters to 289.9 meters. The extent of area ranges from Latitude 29.90°N, Longitude 77.92E and to Latitude 29.83° N, Longitude 77.85° E. The moisture conditions in the area are different in July and March in which the remote sensing data of the study were acquired.

2.2 Remote Sensing Data

Three ERS-2 SAR C- band images (5.3 GHz frequency and VV polarization) at spatial resolution of ~12.5m acquired on 23rd July, 2001, 28th July, 2003 and 29th March, 2004 have been procured from NRSA, Hyderabad. One image from LISS II sensor at spatial resolution of ~36m on board Indian Remote Sensing (IRS) 1B has been acquired to compare the classification accuracy of our algorithm. Topographical map of the same region is also used for reference to check the accuracy of segmentation process. Ground Control Points (GCPs) are chosen from topographic sheet. 5500 GCPs of water and urban areas are chosen for comparison.

* Corresponding author :919897030568

3. ALGORITHM EMPLOYED

3.1.1 Geo-referencing of ERS_2 SAR Image

Since, SAR images are acquired in the microwave region of electromagnetic spectrum, visual identification of ground control points is very difficult. Thus, ERS-2 SAR images have been georeferenced to geographical coordinates using eight ground control points (four at the corners, one at centre of the image and three from topographical map). A first order polynomial transformation function and the nearest neighbour resampling technique have been used to perform georeferencing.

3.1.2 Speckle Suppression

Speckle filtering is applied for speckle reduction, preserving the dominant scattering mechanism of each pixel. Coefficient of variation is calculated for the image and this variable is used to fine tune the speckle suppression filters and this process was carried out using IMAGINE Radar Interpreter.

3.1.3 Segmentation Process

The ERS-2 SAR-C band image acquired on July, 2001 was taken and the segmentation process was employed.

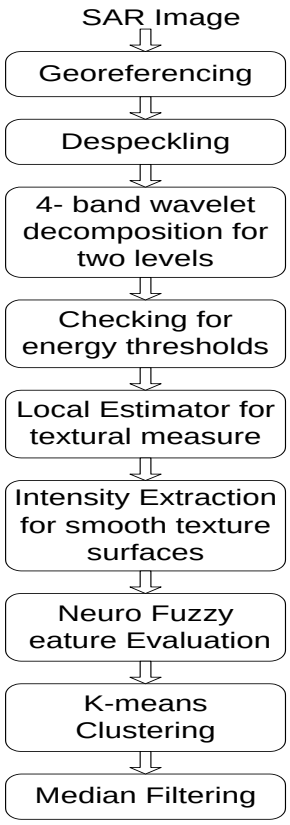

On the geo-referenced and speckled image, 4- band wavelet decomposition with out down-sampling for two levels is applied. The main aim of this wavelet packet decomposition process is to tile the images at different resolution and detect the edges and discontinuities in each of the scale so that texture patterns at all scales are integrated and compiled when reconstructing the image. Four band wavelet filters is so chosen that it has perfect reconstruction ability (Alkin, O., *et al* 1995). One application of 4- band wavelet decomposition on the image gives rise to 16 images and they are termed as subbands at level 1. The 4-band wavelet decomposition is applied on the selected sub bands from level 1 satisfying the above energy thresholds and this gives rise to subbands at level 2. A particular sub band is chosen for consideration or further decomposition only if it contains more than 3% (ε_1) of its parent band energy and has more than 2% (ε_2)of the total energy of all the sub bands at the current level. From the above process of decomposition of the original image into subbands for depth level of 2 and energy checks applied on them, chosen subbands with maximum information contained in them are obtained. Redundancy of information is removed by energy checking. Raw wavelet coefficients present in individual subbands are not sufficient for texture information. Textures are to be characterized by some statistical property linked with it. Here, we are using the variance of the individual pixels from the mean of the pixels considered in a fixed window. The window size must be large such that it is capable of enclosing a single texture pattern or a texel. If larger window sizes are used, it can capture larger texels but introduce errors in the boundary pixels. Level II subbands are the one which are zoomed on to narrower frequency channels so these subbands carry information about the texture variation. Level I subbands are the one which carry a broader information about all the texture patterns, Hence level I subbands are utilized to capture the boundary information and level II subbands for the texture patterns. For a fixed window size of w, the mean of all the pixels around the centre pixel is computed as $\bar{S}(x,y)$. To compute the variation of individual pixels around the centre pixel from the mean, the sum of the absolute values of deviation is considered. This is performed by a local estimator that constitutes a nonlinear operator followed by a smoothing filter is applied to each band, where S_b is the subband image. The textured feature vector, $feat_{tex}$ is given by

$$feat_{tex}(x,y) = \frac{1}{R}\sum_{m=1}^{w}\sum_{n=1}^{w} abs(S_b(m,n) - \bar{S}(x,y)) \quad \text{- (1)}$$

where

R= w^2, w is the row/column size of the window around the central pixel (x,y) over which textural feature vector is calculated.

$\bar{S}(x,y)$ is the subband image averaged over a mask of wxw centred around (x,y)

$abs(S_b(m,n))$ is the absolute value of subband image at (m,n) location.

To identify the smooth texture pattern, the following condition is imposed to get the intensity information also integrated in the feature vector. If the texture is perfectly smooth, then the $feat_{tex}$ =0. To capture the intensity information under such condition

If $feat_{tex}(x,y)$ < threshold (0.001),

$$feat_{int}(x,y) = k * S_b(x,y) + offset$$

else

$$feat_{int}(x,y) = feat_{tex}(x,y) \quad \text{- (2)}$$

where

$feat_{int}$ is the integrated feature vector having both intensity and texture information contained in corresponding subband.

The k factor and offset are introduced only to differentiate the intensity feature from the textural features captured by the integrated feature vector. This is followed by a smoothing stage using Gaussian low pass filter $h_G(x,y)$ to get the feature vector of individual subband images.

$$feat_b(x,y) = \sum_{(a,b)\in G_{x,y}} \Gamma(feat_{int}(a,b)h_G(x-a,y-b)) \quad \text{- (3)}$$

Gaussian window helps in smoothing the results in the sense that it results in less sparse distributions. Empirically, a gamma value of 4 for the Gaussian smoothing filter found to be suitable for the application to SAR images. These feature vectors were ranked according to the information contained in them using Neuro fuzzy feature evaluation index(Acharyya, M., 2001). By choosing the vectors only those are relevant for classification will increase the similarity between the same pair of patterns giving rise to more classification accuracy. Ranking of these chosen features is done by using the neuro-fuzzy feature evaluation algorithm. This is made computationally efficient by computing the cluster centres for the entire feature space [cen_1, cen_2.. .cen_k] for 'k' number of classes. Then, the similarity of individual feature vector spaces with the cluster centre space is computed.

$$\mu_{pc} = 1 - d_{pc}/D, \quad \text{if } d_{pc} \geq D$$
$$= 0, \text{ otherwise} \qquad \text{- (4)}$$

where d_{pc} is the distance between the p*th* pattern and c*th* cluster centre in the feature space and is defined as

$$d_{pc} = \left[\sum_i w_i^2 (x_{pi} - cen_{ci})^2\right]^{1/2} \qquad \text{-(5)}$$

where

w_i = the weighting coefficient corresponding to the ith feature.

X_{pi} and cen_{ci} corresponds to the ith feature of the pth pattern and cth cluster centre respectively.

Back propagation network is chosen for neuro-fuzzy evaluation. The neural network is designed with 3 layers, an input, a hidden and an output layer with 2n nodes in the input layer, n nodes in the hidden layer and 2 nodes in the output layer, where n is the number of feature vectors in the complete feature space, which are to be ranked. All the feature vectors are presented to the network. The weights are updated using the formula,

$$\Delta w_j = -\eta \frac{\partial E}{\partial w_j} \qquad \text{- (6),}$$

where

$$E = \frac{2}{s(s-1)} \sum_p \sum_c \frac{1}{2}\left[\mu_{pc}^T(1-\mu_{pc}^0) + \mu_{pc}^0(1-\mu_{pc}^T)\right] \text{- (7)}$$

where E is the training error

w_j is the weights connecting the jth hidden layer and node T in the output layer.

Neural network is trained till the Δw_j is less than 0.001.E after convergence attains a minimum and then the weights of the links connecting hidden nodes and the output node indicate the order of importance of the features. The ranking of the feature vectors is given by the value of the weighing coefficients. Rank the weighing coefficients connecting n nodes in the hidden layer and μ_{pc}^T and this gives the ranking of the n features. Any 'r' number of features can be chosen according to their rank of importance and given for K-means classifier. For the top ranked features, K-means clustering algorithm is employed to cluster the feature space and segmented image is obtained.

Window size of Local estimator 1	**Classification accuracy (%)**								
	Local estimator 2 window size								
	3	**5**	**7**	**9**	**11**	**13**	**15**	**17**	**19**
3	51.50	57.89	45.20	38.06	59.04	66.99	67.50	67.74	40.05
5	52.66	57.57	57.26	56.10	59.10	61.21	65.51	66.11	43.86
7	52.50	52.73	57.36	58.94	59.30	63.72	63.75	73.55	72.97
9	57.50	66.20	58.99	59.11	59.23	59.28	59.12	59.03	63.80
11	65.96	66.36	65.58	64.68	66.76	63.76	63.61	63.38	63.73
13	64.72	66.46	65.69	64.67	63.72	63.67	63.40	63.33	63.10
15	64.75	66.60	65.72	64.57	63.83	57.05	72.55	72.74	63.01
17	64.82	66.50	65.71	64.53	57.40	59.17	72.53	72.74	54.50

Table 1. Effect of Variation of local estimator 1 and local estimator 2 window sizes on classification accuracy computed for segmented SAR image, 2001 comparing with LISS image

Window size of Local estimator 1	Classification accuracy (%) Local estimator 2 window size								
	3	5	7	9	11	13	15	17	19
3	72.50	79.35	84.57	83.01	73.79	92.37	69.23	98.26	94.10
5	77.68	78.83	81.77	82.70	68.41	85.03	85.96	60.63	64.89
7	81.75	76.60	79.62	82.55	84.15	83.99	83.61	89.13	83.48
9	72.10	82.51	80.66	82.78	84.05	83.89	83.25	82.75	82.46
11	84.61	83.57	81.59	82.62	84.11	83.54	83.01	71.35	70.62
13	81.38	83.87	81.53	82.65	83.85	83.20	82.12	71.06	70.44
15	82.34	83.62	81.10	82.85	83.52	82.81	81.73	81.24	70.13
17	80.92	83.64	81.34	82.96	83.61	82.67	81.52	81.19	82.11

Table 2. Effect of Variation of local estimator 1 and local estimator 2 window sizes on classification accuracy computed for segmented SAR image, 2001 comparing with topographic sheet (5500 GCPs)

4. RESULTS AND DISCUSSION

There are many user defined parameters such as ε_1, ε_2 for sub band selection, window sizes of local estimator 1, local estimator 2 and number of features selected from neuro fuzzy algorithm. These user defined parameters are to be optimised for good classification accuracy. Initially, the effect of these user defined parameters on classification accuracy is studied by varying the parameters individually. Then, optimum values of these parameters are decided. To evaluate the classification accuracy of the segmented image obtained by our algorithm, LISS image and topographic region of the same region are considered. For the LISS image, supervised classification by maximum likelihood classifier is performed with the help of topographical sheet.

The SAR image of the region (year 2001) considered has 36.11% of water and 13.45% of urban area. The same region has: water: 30.5% & urban: 13.53% in 2003 and water: 24.6% & urban: 13.57% in 2004. The water and urban area percentage is projected here to specify that the algorithm with optimum parameters mentioned in this paper work for any SAR area with sites having this proportions of urban and water areas. The segmented image is evaluated by considering only the water and urban pixels in the image. The above methodology of segmentation is performed on the SAR image (2001) by varying the window sizes for local estimator 1 and 2 from 3 to 17 and 3 to 19 respectively. Classification accuracy is computed by comparing it with LISS image. For comparison with topographic sheet of the same region, 5500GCPs (Ground control points) are considered. Table 1 and 2 lists the classification accuracy obtained for varying values of window sizes of local estimator 1 and local estimator 2. From the above tables 1 and 2, we can see that particular combinations of local estimator 1 and 2 are providing good classification accuracy. Some combinations like [7, 15], [7, 17], [13, 15], [13, 17] and [15, 13] are chosen and the number of feature vectors are varied from 2 to 27 to study the effect of variation of number of feature vectors on classification accuracy. Similarly, the number of feature vectors is varied from 2 to 27 and the segmented image is compared with the 5500 GCPs in the topographic sheet. Table 4 lists the variation of classification accuracy with the number of feature vectors for the same chosen combinations for window size of local estimator 1 and local estimator 2. If the statistics obtained from the LISS image alone is considered, then, the combinations of the user defined parameters for obtaining good classification accuracy is [7,17,11] for window size of local estimator 1, window size of local estimator 2 and number of feature vectors.

Number of feature vectors	Classification accuracy (in %) Local estimator 1 and 2 window sizes				
	7,15	7,17	13,15	13,17	15,13
2	56.72	54.53	56.71	51.93	33.10
4	57.70	58.03	59.65	67.40	67.40
6	59.33	64.37	62.42	62.78	59.34
8	62.83	62.46	61.91	62.65	59.30
10	64.05	61.60	63.84	64.00	65.00
11	63.75	73.55	63.40	63.33	67.05
12	63.77	63.88	63.44	63.39	63.64
14	63.84	64.00	63.50	63.44	59.30
16	60.00	60.00	58.96	59.00	59.30
18	59.50	62.38	58.95	58.89	59.18
21	59.30	62.28	59.05	58.88	59.20
27	59.30	62.18	55.93	58.87	59.20

Table 3. Classification accuracy for different numbers of feature vectors by comparing with LISS image

Number of feature vectors	Classification accuracy (in %) Local estimator 1 and 2 window sizes				
	7,15	7,17	13,15	13,17	15,13
2	74.70	75.65	74.78	60.28	70.97
4	74.33	73.64	68.85	65.84	82.42
6	80.82	77.45	67.18	67.34	82.24
8	83.61	83.21	82.04	82.92	82.56
10	68.62	69.71	69.39	69.25	82.53
11	83.61	89.13	82.12	71.06	82.81
12	82.36	70.48	82.17	71.24	82.82
14	82.83	71.25	81.94	72.28	82.55
16	82.74	70.89	82.07	71.69	82.79
18	82.98	90.16	71.13	71.59	82.81
21	83.98	90.2	70.96	81.33	82.57
27	83.96	84.59	71.04	81.22	82.55

Table 4. Classification accuracy for different number of feature vectors by comparing segmented image with topographic sheet

Comparison with LISS image alone is considered since it gives an estimation of the goodness of overall accuracy that can be obtained by the segmentation process. It is obvious from Table 3 that as the number of sub bands increases, the classification accuracy also increases and it reaches a maximum at number of sub bands= 11 (for the combination of local estimator 1=7 and local estimator 2= 17) and then reduces for further increase in the number of sub bands. It is also obvious that other combinations of local estimator1 and local estimator 2 like (7, 15), (13, 15), (13, 17) and (15, 13) have not produced better results than the chosen combination (7, 17) even by varying the number of sub bands.

From the tabulated values obtained for classification accuracy for varying number of sub bands, an empirical relationship is developed. By curve fitting method, a fourth degree polynomial is fitted to the data in Table 3, thereby developing a relation between the number of sub bands and the classification accuracy.

$$\% \text{ accuracy (acc)} = p_1 b^4 + p_2 b^3 + p_3 b^2 + p_4 b^1 + p_5 \quad (8)$$

where b is the number of sub bands.

The coefficients p_1, p_2, p_3 and p4 are obtained as -0.000106, 0.01155, -0.3895, 4.796 and 45.76 respectively giving the coefficient of determination, R^2 of 0.7225.

From this empirical relationship, the number of sub bands required for achieving maximum classification accuracy can be obtained.

Condition for maximum accuracy is d(acc)/db=0 and $d^2(acc)/db^2$ = negative.

By applying this condition, we find that for all the selected combinations of the local estimator 1 and 2 in table 4, the optimum number of sub bands is 11 (rounding off to integer). Developing this empirical relationship helps in identifying the number of sub bands required for obtaining maximum classification accuracy that can be obtained by the system.

Sl.No	User defined parameters	Producer's accuracy(%)		User's accuracy(%)	
		Water	Urban	Water	Urban
1	7,15,11	62.76	59.6	30.84	69.16
2	7,17,11	66.47	100.0	100.0	84.79
3	13,15,11	61.96	100.0	100.0	82.66
4	13,17,11	64.19	100.0	100.0	80.35
5	15,13,11	73.14	100.0	100.0	84.99

Table 5. Classification accuracy of the SAR image taken on 28, July 2003

Sl.No	User defined parameters	Producer's accuracy (%)		User's accuracy (%)	
		Water	Urban	Water	Urban
1	7,15,11	75.88	36.99	66.08	91.26
2	7,17,11	99.73	100.0	100.0	99.87
3	13,15,11	62.66	99.74	99.74	62.54
4	13,17,11	60.88	100.0	100.0	82.25
5	15,13,11	65.26	98.96	98.77	69.03

Table 6. Classification accuracy of the SAR image taken on 29, March 2004

From the study of the variation of the user defined parameters on classification accuracy, optimum values of the user defined parameters are computed as 11 for number of feature vectors, (7,15) for local estimator 1 and 2. By applying this optimum number of combinations of user defined parameters in the segmentation process the classification is applied and mapped the water and urban areas. The same parameter values obtained can be used for the segmentation of the same area obtained at different time instants also.

The above tables show the results by comparing it with topographic sheet. Producer's accuracy is the ratio of total number of pixels reported by the process to the total number of pixels available in the class. User's accuracy is the ratio of total number of correctly reported pixels to the total pixels reported by the segmentation process corresponding to that class. High values of user's accuracy indicate the reliability of predicted results. High values of producer's accuracy indicate the ability of the segmentation process to predict all the areas corresponding to the class. From the table 5,sl.no.2 we can infer that all water areas identified are correct but not all water areas have been identified and only 66.47% are identified correctly for the year 2003. From the table 6, sl.no.2 , we can see that same combination gives satisfying producer and User accuracy for both water and urban areas.

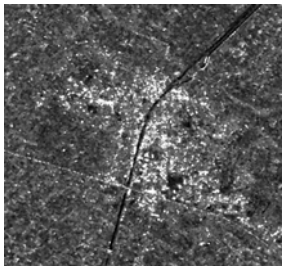

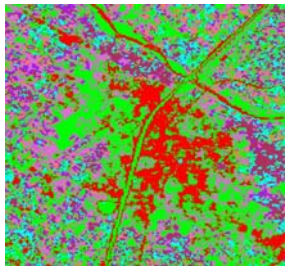

Fig (a) Fig (b)

Fig (a) and (b) corresponds to the original SAR image and segmented LISS image considered for comparison

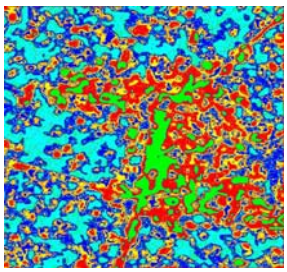

Fig (c) Fig (d)

Fig (c) corresponds to the segmented SAR image for the combination of parameters window size of local estimator 1= 7, window size of local estimator 2 =17, number of feature vectors =11 Fig (d) is the topographic sheet of the same region.

In fig (c) and (d), green corresponds to water area and red corresponds to urban area. The water area (in blue) in the topographic sheet corresponds to the Ganga canal. From the above figures, it is obvious that our segmented process produces agreeable result with both LISS Image and topographic sheet.

5. CONCLUSION

Single band, single polarized SAR image of the Haridwar region of India considered, the optimum number of sub bands is computed as 11 and the corresponding sizes for local estimator 1 and 2 are 7 and 17 respectively. This set of optimum parameters is applied and segmentation was performed on the image. The optimum values are obtained directly from the empirical relation given. Water and Urban areas are compared with the LISS image and topographic sheet. Overall accuracy is the ratio of correctly identified urban and water pixels to the total urban and water pixels present in the image. The optimum parameters are site-specific and it can be applied to the image of the same region obtained at different time instants. The methodology presented in this paper gives an efficient methodology for unsupervised segmentation of SAR images.

ACKNOWLEDGEMENT

Authors are thankful to Ministry of Human Resource and Development (MHRD) of India to provide fund to support this work.

REFERENCES

Chang, T.,and Jay Kuo, C.C., 1993. Texture analysis and classification with tree-structured wavelet transform. In: *IEEE Transactions on Image Processing,* vol. 2, no. 4, pp. 429-441.

Clausi , D.A., and Jernigan, M.E., 1998. A fast method to determine co-occurrence texture features. In: *IEEE Transactions on Geoscience and Remote Sensing*, vol. 36, no. 1, pp. 298-300.

Haralick, R.M., 1979. Statistical and structural approaches to texture. In: *Proceedings of IEEE*, vol.67, no. 5, pp. 786-804.

Jain, A.K., and Farrokhnia, F., 1991. Unsupervised texture segmentation using Gabor filters. In: *Pattern Recognition*, vol. 24, no. 12, pp. 1167-1186.

Lindsay, R.W, Percival, D.B. and Rothrock, D.A., 1996. The discrete wavelet transform and the scale analysis of the surface properties of sea ice. In: *IEEE Transactions on Geoscience and Remote Sensing*, vol. 34, pp. 771-787.

Manjunath, B.S., and Chellappa, R., 1991. A Note on unsupervised texture segmentation. In: *IEEE Transactions on. Pattern Analysis and Machine Inteligence,* vol. 13, no. 5, pp. 478-483.

Manjunath, B.S., and Ma, W.Y., 1996. Texture features for browsing and retrieval of image data In: *IEEE Transactions on. Pattern Analysis and Machine Inteligence,*vol. 18, no. 8, pp. 837-842.

Acharyya, M., Rajat K.De and Malay K.Kundu, 2000. Segmentation of remotely sensed images using wavelet features and their evaluation in soft computing framework. In: *IEEE Transactions on Geoscience and Remote Sensing*, vol. 41, no. 12.

Acharyya, M., and Malay. K.Kundu., 2001. An adaptive approach to unsupervised texture segmentation using M-Band wavelet transform. In*: Signal Processing 81*pp. 1337-1356.

Mecocci, A., Gamba, P., Marazzi,A.,and Barni, 1995.Texture segmentation in remote sensing images by means of packet wavelets and fuzzy clustering. In: *Proceedings of SPIE European Symp. Satellite and Remote Sensing II*, vol. 2584, pp. 142-157.

Oktay Alkin and Hakan Caglar, 1995. Design of efficient M-Band coders with linear phase and perfect reconstruction properties. In: *IEEE Transactions on Signal Processing*, vol. 43, no. 7.

Randen, T., and Husey J.H., 1999. Filtering for texture classification: A comparative study. In: *IEEE Transactions on. Pattern Analysis and Machine Inteligence*, vol. 21, no. 4, pp. 291-310.